Chapter

Hard Alloys with High Content of WC and TiC—Deposited by Arc Spraying Process

Stefan Lucian Toma, Radu Armand Haraga, Daniela Lucia Chicet, Viorel Paleu and Costica Bejinariu

Abstract

Obtained by different spraying technologies: in atmospheric plasma spray, High Velocity Oxygen Fuel (HVOF) or laser cladding, the layers of hard alloys with a high content of WC and TiC find their industrial applications due to their high hardness and resistance to wear. Recognized as being a process associated with welding, the arc spraying process is a method applied industrially both in obtaining new surfaces and for reconditioning worn ones. This chapter presents the technology for obtaining ultra-hard layers based on WC and TiC - by the arc spraying process, using a classic spray device equipped with a conical nozzle system and tubular wire additional material containing ultra-hard compounds (WC, TiC). To study both the quality of deposits and the influence of thermal spray process parameters on the properties of deposits with WC and TiC content, we approached various investigative techniques, such as optical scanning microscopy (SEM), X-ray diffraction, and determination of adhesion, porosity, Vickers micro-hardness and wear resistance.

Keywords: arc spray process, ultra-hard alloy, wear, WC, TiC

1. Introduction

There is a multitude of technological processes that allow the modification of the physico-chemical and mechanical properties of the surfaces in order to increase the performance in operation, the service life, or the esthetic aspect, [1–3].

The improving the surface properties, by thermal spraying, is carrying out by depositing new materials on the existing surface in order to give it new properties. Therefore, „thermal spray" is a general term that groups a set of processes, by which a material is melted under the action of a heat source, then is projected using a carrier gas on the surface of a part [4–6].

Coating via thermal spraying consists of the acceleration of fine particles from a certain metallic material, in a molten or semi-molten state, onto a specially prepared surface. The sprayed material is called coating material (CM) and the surface on which the deposition is made is called substrate (S), [7–10]. The layer produced by thermal spraying becomes a constituent part of the base material and gives it specific properties: hardness, corrosion resistance, wear resistance or new functional properties (chemical, electrical, magnetic).

1.1 Background

Depending on the melting method of the coating material, the thermal spraying processes can be classified into four main categories, as presented in **Figure 1**.

The thermal spraying processes are realized with the help of installations and equipment capable to develop the necessary heat for the CM melting, to achieve the dispersion of the formed droplets into fine particles and to transfer to them kinetic energy.

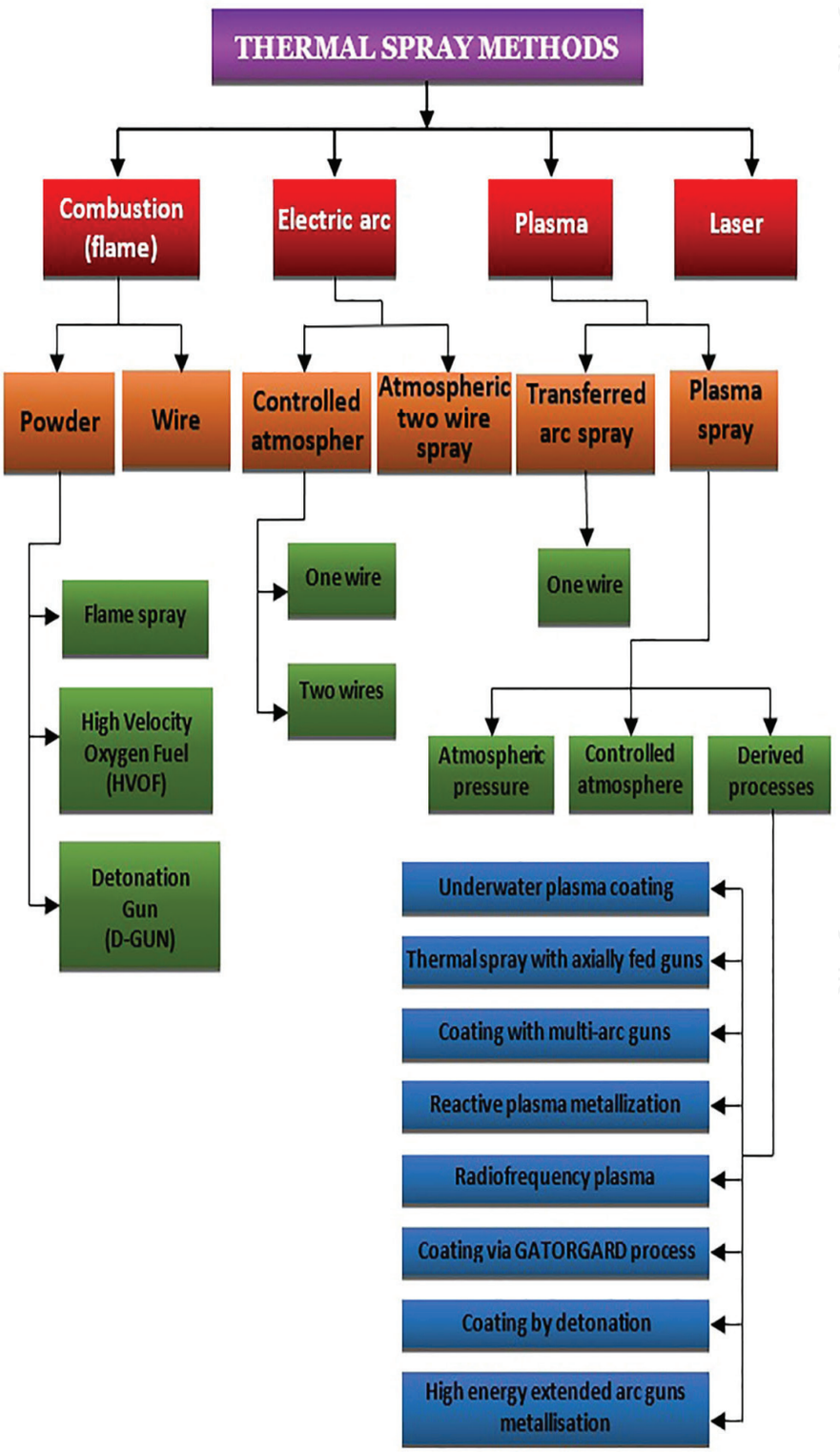

Figure 1.
Classification of thermal spray methods, [11].

The substrate material can be of any nature: ferrous, non-ferrous, plastic, ceramic, textile, glass, wood, but the coating material is limited by its capacity to be transformed into a liquid state, or to be processed into of powder, wire, cord or wand, [12–13]. Usually, spraying processes allow the deposition of a diverse range of materials: pure metals and metal alloys, cermets, ceramics and under certain conditions polymers, [2, 14, 15].

The thermal spraying methods, recognized in the specialized technical literature as synergetic and versatile [16], have as objectives:

- production of new layers, with physical, chemical, mechanical and technological properties different from those of the substrate;
- restoring the geometry of some parts with a high wear degree;
- obtaining pulverulent products used in different industrial sectors (sintering, spraying).

Recognized as the cheapest process for obtaining spray coatings, two-wire arc spraying finds numerous industrial applications that aim to obtain both surfaces with new properties and the restoration of used surfaces. [11–13].

The spraying method consists of making an electric arc between two consumable metal wires, followed by the atomization of the molten material with the help of a compressed air jet and the spraying of those particles on the substrate surface - **Figure 2**, [17]. Although the functional principle constructive of electric arc spraying devices is apparently simple, it must to allow the correlation between the wire feed speed, the intensity of the electric current in the circuit and the pressure of the compressed air, in the purpose of obtaining qualitative coatings and maximum yield, [11].

The electric arc coating devices also called spraying guns, are powered by direct current generators which have a rigid characteristic, develop voltages between 25 and 45 V and high currents with values in the range of 100–500 A, [18]. They are characterized by a modulated design, composed of:

- the wire entrainment device, also called the wire feed mechanism - according with SR EN 657/1995 standard;
- melting-spraying module, known as "spray head" - according with SR EN 657/1995 standard.

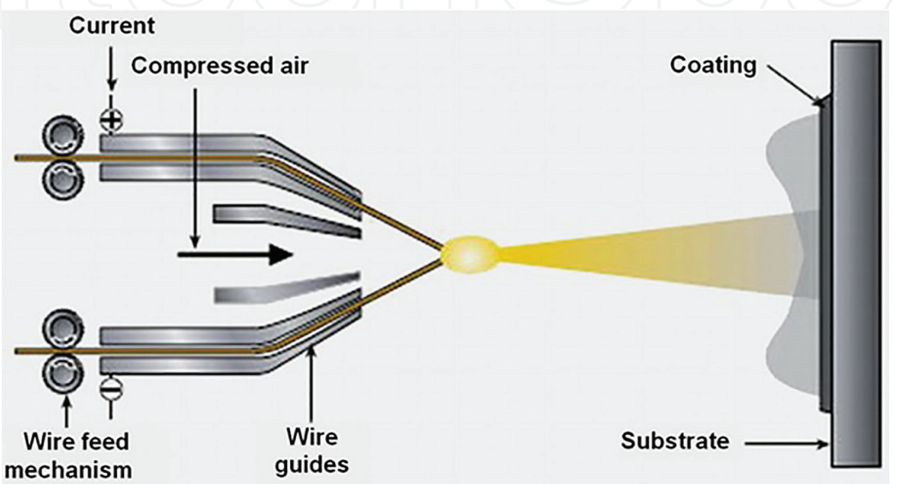

Figure 2.
Schematic representation of electric arc coating method, [17].

The wire feed mechanism is positioned directly on the gun or outside of it and has the role of directing the wire from the coils towards the area of electric arc formation.

The spray head includes the wire guides and the nozzle through which the compressed air passes - symbolically called carrier gas, [2]. During the device functioning, the nozzle is placed in the lower part of the melting zone, before the contact point of the wire electrodes, usually called "arc point". The role of the spray head is to direct the entrainment gas in the area where the electric arc is formed, in order to produce the division (atomization) of the droplet of molten filler material into particles, which it propels on the surface of the substrate, [19].

The dispersion of the molten droplets determines the interrupting of the circuit respectively of the electric arc. The electric arc priming is carrying out by advancing the wires in the melting area, where the medium is strongly ionized. The phenomenon has a periodic character, being composed of melting sequences of the input material followed by interruptions. In this case, the electric arc is a short-circuit arc, intermediate between the usual arc and the "breaking" arc produced at the interruption of a circuit, [20, 21].

1.2 State of art

The formation of coatings by thermal spraying in electric arc is carried out according to a well-precisely mechanism, presented in **Figure 3**, composed of the following stages, [18]:

- heating the coating material, used as wire;
- forming a drop of molten material;
- transformation of the coating material into fine particles - atomization;
- displacement of the melted particles towards the surface of the substrate;
- the impact of the particles with the surface of the substrate;
- coating formation by successive particles depositions.

Each stage is accompanied by a series of physical phenomena and interactions, such as: sequential melting of the coating material by Joule - Lentz effect; interaction between gas and molten metal, having as result the droplet dispersion ("atomization"), in micron size particles; propelling the particles formed onto the surface of the substrate; particle-substrate interaction (impact); solidification of the sprayed particles, [22].

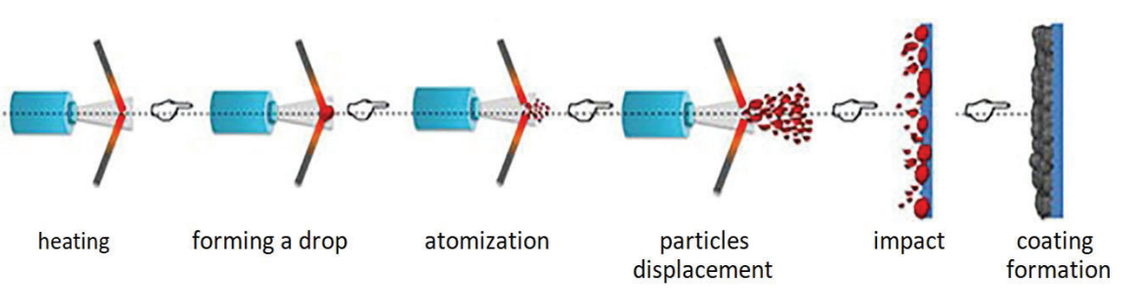

Figure 3.
Coatings formation mechanism by electric arc thermal spraying.

The interaction between the molten metal and the uninsulated jet of gaseous fluid, under pressure, at ambient temperature, has as effect the heat transfer by forced convection between droplets (particles) and jet, fact which can determine the apparition of rapid solidification phenomenon in the droplet (particle).

It is known that the properties of the coatings produced by electric arc thermal spraying are closely related to the velocity and the temperature of the particles before the impact [23, 24]. The two parameters that characterize the particles from a thermodynamic point of view are mainly influenced by the intensity of the electric arc and the pressure of the carrier gas flow. The intensity of the electric current determines the melting/overheating temperature of the filler material. The carrier gas pressure, in close connection with its velocity, influences the displacement velocity of the particles towards the substrate surface [25, 26].

The studies carried out by Zhao et al. [27], on the flow phenomenon of an uninsulated gas jet which pass through a nozzle, demonstrates the fact that the velocity and the temperature of the gaseous fluid decrease continuously along the jet. Due to the interaction between the fluid and the sprayed particles, it can be said that the molten particles inside the spray jet have a transient behavior, characterized by the continuous decrease of speed and temperature.

A large category of ductile metal materials, such as: aluminum, zinc, copper, bronze, steels as well as numerous wire drawing alloys can be sprayed by this technique, [28]. The exploitation of high temperature of the electric arc directed the scientific research towards the extension of the input materials range of use, by removing the technological barrier imposed by electrical ductility and conductivity. Thus, appeared the tubular wires, which have the exterior formed by a metal mantle characterized by high conductivity, and the interior is filled with powders of fragile materials, [29]. Recently, have been developed wires manufacturing technologies by crimping, in which the ductile material is folded and inside the folds are injected powders of hard materials. [30]. The widening of the spectrum of use of the input materials determined that the arc spraying process to be competing with the other spraying techniques (plasma, flame) in the technology of restoring of large surfaces.

The advantages of the arc spraying process are [2, 18]: efficiency - from an energy point of view (power used between 5 ÷ 10 kW), high productivity (15 ÷ 45 kg/h), no need to preheat the substrate, uses cheap equipment compared to other spraying processes.

The main disadvantages of this spraying process are related to the high porosity of the deposits (over 18%) and to carrying out deposits resistant to abrasive wear (WC, TiC) only by using high-performance equipment, equipped with command and control system, which are expensive, [31].

The purpose of our research is to present the technology of obtaining coatings of alloys resistant to abrasive wear - containing ultra-hard chemical compounds (WC and TiC), arc thermal the process using a classic spray device provided with a system of conical nozzles and tubular wire with a containing ultra-hard compound (WC and TiC), as additional material.

The objectives of our study are the following:

- the realization of a system of conical nozzles able to melt the additional material (which contains ultra-hard compounds: WC and TiC) and to transfer, to the formed particles, the high speed necessary to obtain dense coatings,

- the characterization of the ultra-hard alloys coatings obtained with the aforementioned spraying device equipped with the conical nozzle system,

- establishing the optimal process parameters.

2. Preparation and characterization of deposits

In order to carry out our own research on the possibility of obtaining ultra-hard coatings based on WC and TiC by thermal spraying, we made a spraying head system, which we have adapted to a classic drive mechanism, [32]. The schematic overview of the spraying device is presented in **Figure 4**.

The designed spray device consists of two distinct modules:

- wire feed module;
- spraying module.

The wire feed mechanism - realized by IOR Bucharest, Romania, consists of a direct current electric motor, two-step speed reducer (vertical stage) and electronic control system. It develops at the output a power P_{ie} of 0.063 kW and a speed n_{max} of 10 rpm. The overview of the wire feed mechanism is shown in **Figure 5**.

The spray module (usually called "spray head") is designed from a system of concentric nozzles - see **Figure 6**, convergent at the electric arc level, capable to ensure a convergent – divergent geometry, of the compressed air jet.

The components elements of the nozzle system are made of insulating materials such as: textolite, high density polypropylene and polyurethane of Moldotan type.

The concentric nozzle system, together with the module body, forms two compressed air circuits [32, 33], as presented in **Figure 7**:

- the main circuit - formed in the space between the module body, the conical nozzle with grooves and the conical insulator;
- the secondary circuit - formed in the space between the cover, the front nozzle, the conical nozzle with grooves and the body of the module.

The compressed air which passes through the *main circuit* determines the detachment of the liquid droplets from the wires surface and the dispersion of the droplet formed into fine particles. This circuit influence thus the size and the speed of the sprayed particles, [32]. The compressed air that passes through the secondary circuit has the role of constraining the electric arc, determining the increase of the current density and implicitly of the particle temperature. It is directed by the inner surface of the constraint frontal nozzle - see **Figure 8**, to the forming area of the electric arc. The two compressed air circuits are supplied from two different sources, with different pressures.

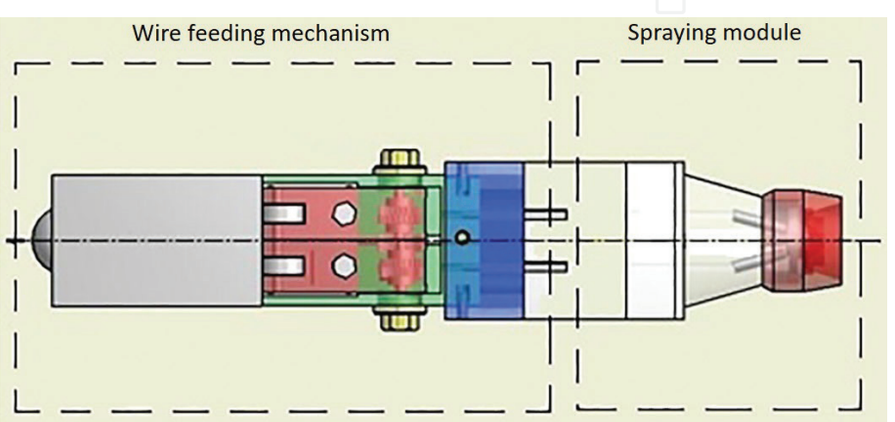

Figure 4.
Spray device - schematic overview.

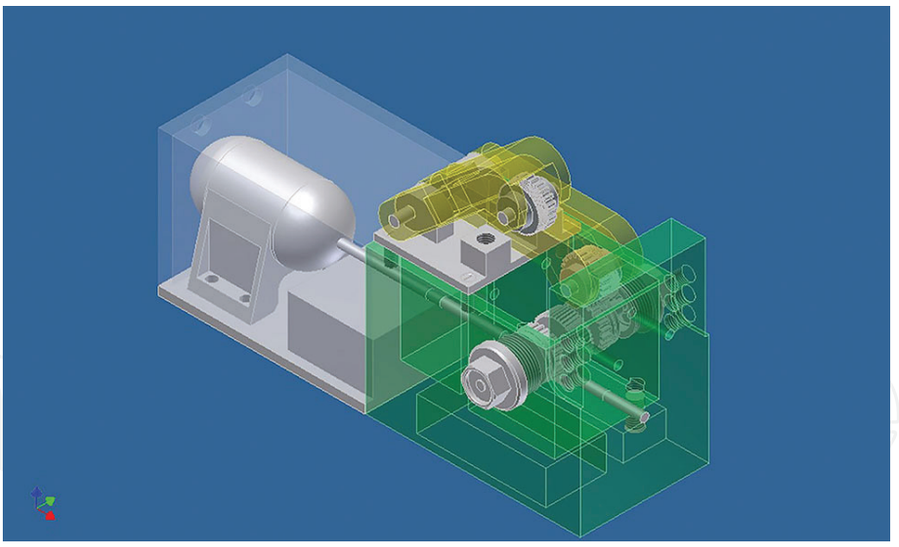

Figure 5.
Wire feed mechanism assembly.

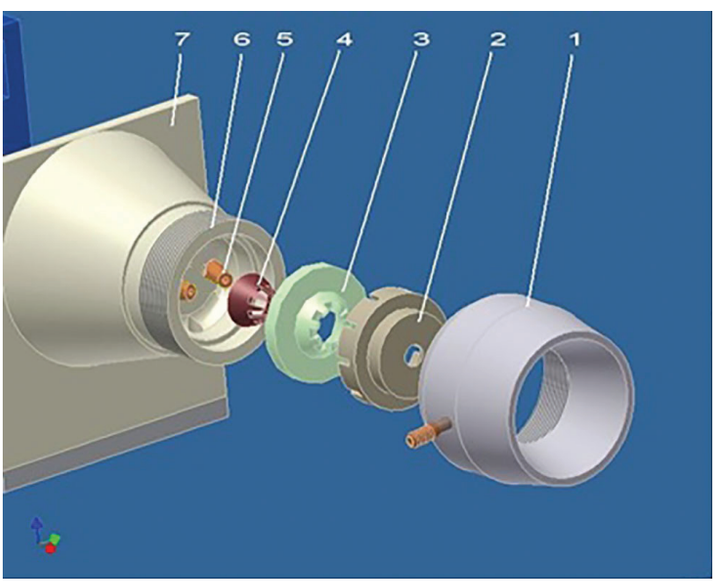

Figure 6.
Spray head: Isometric view - exploded:1- front cover; 2-front nozzle; 3-conical nozzle with grooves; 4- conical insulator; 5-wire guides; 6-thread; 7-module body.

2.1 Technological workflow

In our research substrates made of low alloy steel C15 –EN10083, with dimensions of 40 mm x 40 mm x 10 mm were covered by arc spraying process using as additional material 97MXC - in the form of cored wires, product of the company Praxair-Tafa, USA. The chemical composition of the substrate, as well as that of the additional material is presented in **Table 1**.

In order to produce the ultra-hard coatings with WC and TiC content, we used an electric arc spraying installation, provided with a compressed air compressor, which ensures pressures of 8 bar and a flow of up to 700mc/min, a direct current source RSC 400 type and the spray device presented in **Figure 4**.

The stages of the technological flow are schematically presented in **Figure 9**, [11].

The substrate surface activation included a series of preparatory operations for the metallization stage, which aimed both to clean the surface from oxides, oils and

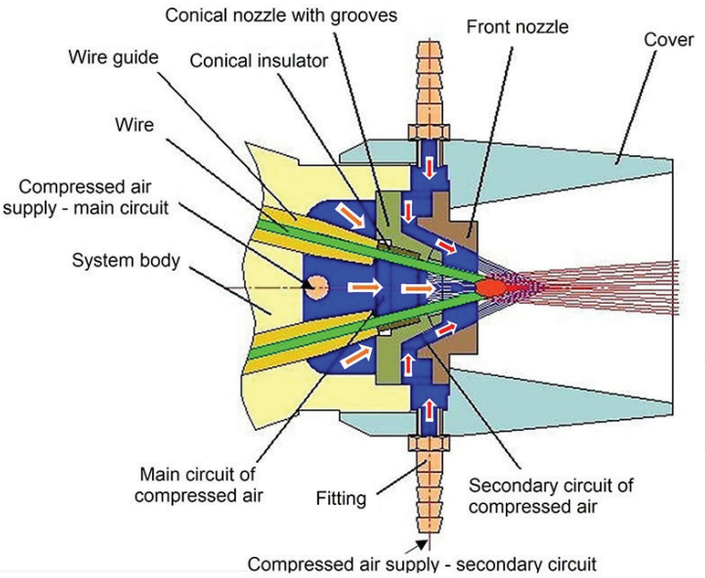

Figure 7.
Operating diagram of the spray head, [32].

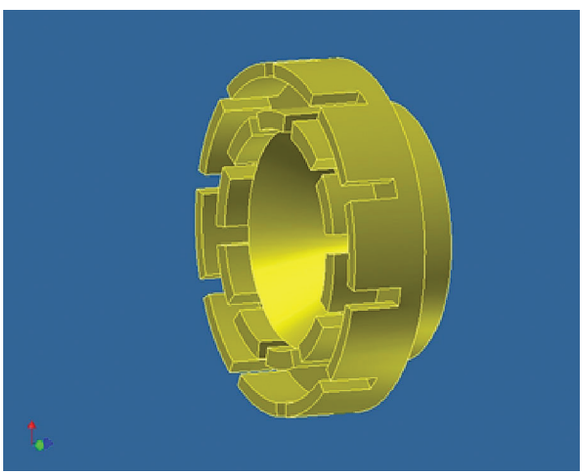

Figure 8.
The frontal constraint nozzle, [32].

Materials	Elements (wt%)										
	C	Si	Cr	Ni	Mn	B	WC	TiC	Fe	P	S
C15	0,14	0,15	0,3	0,3	0,43	—	—	—	—	0,04	0,04
97MXC	—	1,25	14,0	4,5	0,55	1,87	26,0	6,0	balance	—	—

Table 1.
Chemical composition of the materials.

greases, and to increase its roughness, in order to ensure good adhesion of the coating to the substrate, [32, 34]. The surface cleaning operation was performed in two successive phases: chemical cleaning and mechanical cleaning.

Chemical cleaning consisted of several steps: washing the substrate surface in a jet of liquid solution with a concentration of 10% (5% caustic soda, 5% soda salt), at a temperature of 50°C; rinsing in a stream of hot water at a temperature of 90°C; degreasing in methylene tetrachloride; wiping the substrate surface until dry with a textile material, [31].

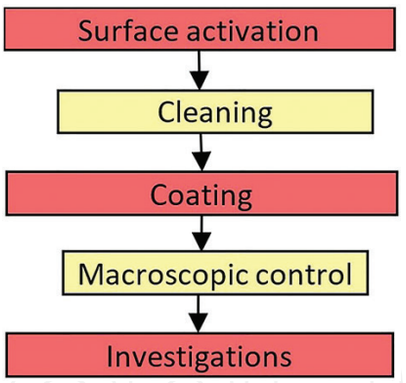

Figure 9.
Technological workflow.

Parameters	Value
Current intensity (A)	200/220/250
Voltage (U)	32
Air pressure in the primary circuit (bar)	5.5/6.0/6.5
Air pressure in the secondary circuit (bar)	3.0
Movement speed of the gun (m/s)	0.14
Coating thickness (mm)	0.5–0.7
Stand-off distance (SOD) (mm)	110

Table 2.
Thermal spray parameters.

The subsequent phase, respectively the mechanical cleaning, consisted in sandblasting the surface of the substrate with abrasive particles. This process required pressurizing the abrasive medium with the help of compressed air and directing the flow of abrasive particles on the surface of the substrate [35]. Hard, abrasive and sharp particles of aluminum oxide with an average diameter of 536 ± 124 μm, sprayed with a pressure of 4barr at a distance of 30 mm, were used for blasting. The surface roughness obtained was between 46 and 62 μm. However, sandblasting always carries great risk, respectively it leaves the surface of the substrate contaminated with abrasive particles entrapped in the material, [36–38]. These residues have negative effects on the mechanical properties of the coatings, such as: they reduce the adhesion of the layer to the substrate, reduce the fatigue resistance properties of the substrate, limits the diffusion between coating and substrate and reduces the contact surface between particles [39–41]. To prevent the mentioned aspects, the substrate surface was ultrasonically cleaned by immersing the specimens in an ethanol bath (C_2H_6O) for 10 minutes, followed by drying them under a jet of filtered compressed air.

In our research, two process parameters, respectively: the compressed air pressure passing on the primary circuit and the intensity of the electric current, varied on three levels. For a good analysis of the effect of these variations, the rest of the technological parameters were kept constant. **Table 2** shows the parameters of the electric arc thermal spray process.

2.2 The characterization of ultra-hard 97MXC coatings

This subchapter presents the following investigations performed for the analysis of the WC/TiC ultra-hard coatings obtained by arc spraying process:

- elementary chemical composition - necessary to determine the presence and the proportions of the chemical elements of the analyzed coatings;
- structural characterization - necessary for the study of microstructure, identification of phases and constituents;
- mechanical characterization - which highlights the mechanical properties of 97MXC coatings: porosity, adhesion, microhardness, wear behavior.

2.2.1 The characterization of ultra-hard 97MXC coatings

A complete characterization of a deposit requires the most accurate knowledge of its chemical composition, the concentration of various alloying elements or impurities. The chemical composition of the 97MXC deposits was determined by semi-quantitative elementary chemical analysis of EDX type (Energy Dispersive X-ray Spectroscopy). The analysis system used (EDAX-AMETEK, Holland, 2008) is attached to an electron microscope (QUANTA 200 3D, FEI, Holland, 2008), being a microanalysis detector that records the energy of X-rays emitted from the surface of the specimen when scanned with an electron beam. This laboratory investigation allowed us to highlight the types of existing chemical elements and the proportions in which they are present.

To determine the chemical composition of the sprayed hard alloys, each sample - measuring 10 mm x 10 mm x 5 mm, was investigated by spot analysis, at 10 different points located on the cross-section. Before being investigated, the samples were metallographically prepared, by sanding on abrasive paper and polishing to remove impurities and oxides formed on the surface of the deposits.

Table 3 presents the mass percentages of the chemical elements identified in the composition of the ultra-hard deposit - depending on the intensity of the electric current used in the thermal spraying process.

As an example, **Figure 10** presents the EDX spectrum and the mapping (distribution of chemical elements on the scanned surface) of the chemical elements present in the 97MXC layer deposited by arc spray process, at current I = 220A and pressure p = 5.5 bar.

In all the cases (of coatings at different intensities with 97MXC material) on the scanned areas, the following chemical elements were identified following the EDX elemental chemical analysis: Fe, W, Cr, C, O Ni and Ti. Correlating these results with the data in **Table 3**, it had been able to conclude that the concentration of the alloying elements does not show changes due to the increase of the electric current intensity, respectively of the increase of the electric arc temperature.

2.2.2 The XRD analysis of the 97MXC coatings

The XRD analysis (XRD - X-ray diffraction) is a fast-analytical technique, used primarily for phase identification of a crystalline material. This type of analysis

Current intensity, (A)	Chemical element, (% weight)						
	Fe	W	Cr	C	O	Ni	Ti
200	48.67	13.84	13.08	11.43	5.63	4.21	3.14
220	48.89	13.64	12.30	12.10	8.65	3.85	2.57
250	46.42	14.21	12.84	12.42	7.32	3.91	2.88

Table 3.
Chemical composition of the ultra-hard coatings (p = 5,5 bar).

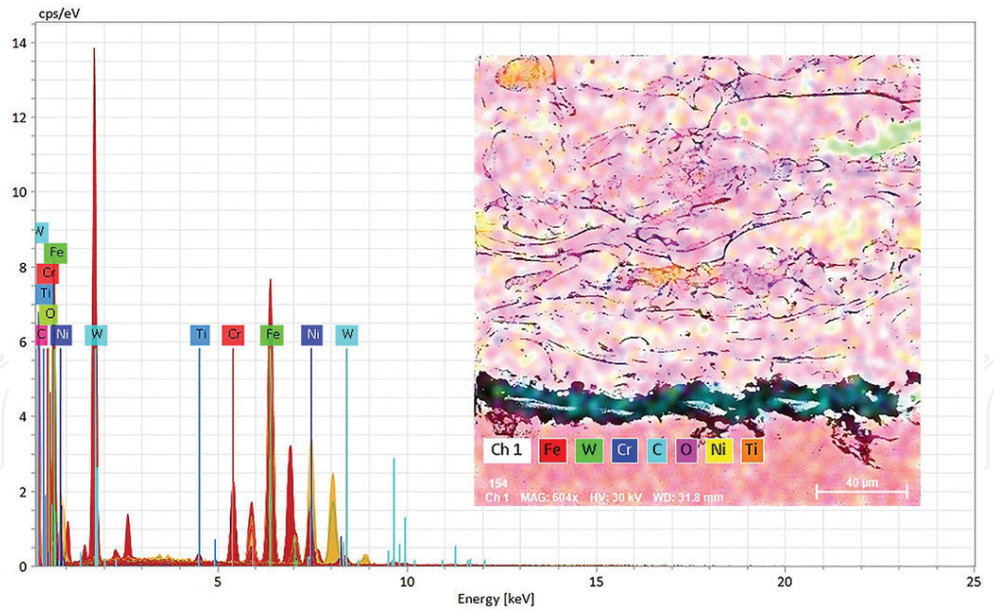

Figure 10.
EDX spectrum and chemical elements distribution map in case of 97MXC coating (I = 220A, p = 5.5 bar).

is very important because it highlights the existing phases and constituents in the electric arc coated layer. Knowing the phases and constituents can help to understand the coatings behavior during the different types of tests they have been subjected to. The testss were performed using the X'PERT PRO MRD diffractometer (Panalytical, Holland, 2008) with the following working configuration: Cu anode with λ = 1.54 Å, open eulerian cradle sample support, 2θ = 20–90°, [42].

Figure 11 shows the X-ray diffraction patterns of the 97MXC coatings obtained at a pressure of 6.0 bar, at a spray distance of 110 mm and different intensities of the electric current: 200 A - sample Ia, 220 A - sample Ib and 250 A - sample Ic.

From the XRD patterns it is observed that the three coatings contain the Fe-Cr alloy, complex carbides of the FeW_3C, Fe_3W_3C and Fe_6W_6C type and fractions of

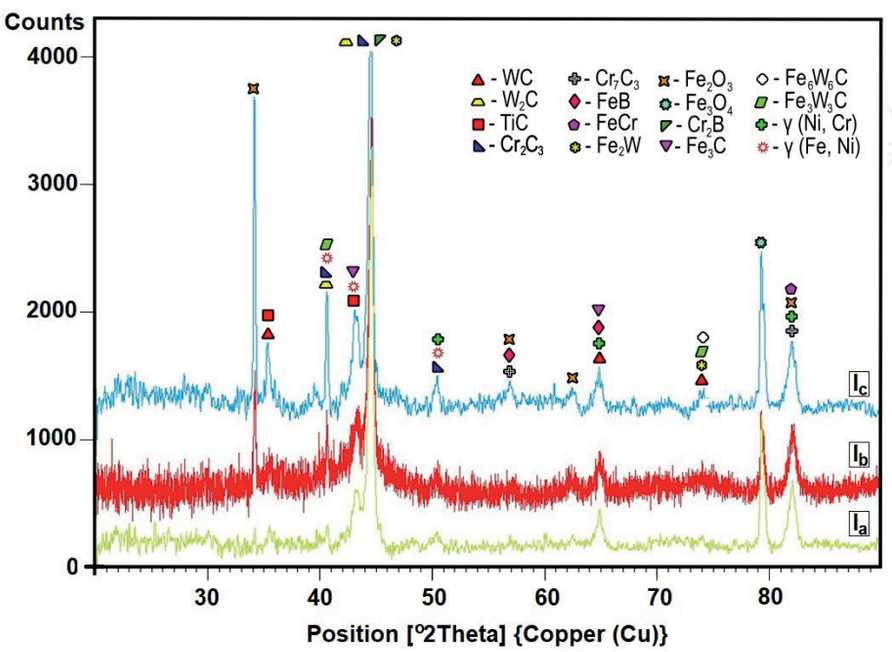

Figure 11.
X-ray diffraction patterns of 97MXC coatings.

FeB, Cr_2B, Fe_2O_3 and Fe_3O_4. Peaks of WC and W_2C are present in all three coatings, formed as a result of decomposition during the thermal spraying process, similar to the results reported by He et al. [43]. In additional to the eutectic phases of WC, W_2C and TiC, alloyed solid solutions of γ(Fe, Ni) and γ(Ni, Cr) were also identified. It is noted that the intensity of the W_2C peak increases with increasing current intensity. It is also suggested that the high temperature of the electric arc favors the decomposition of the WC carbides into single elements, respectively the formation of C-poor compounds such as W_2C.

2.2.3 Structural characterization of the 97MXC coatings

The morphology and metallographic structure of 96MXC deposits were investigated on micrographs obtained using the FEI - Quanta 200 3D scanning electron microscope (SEM). The investigations were performed on the cross section. The samples, measuring 10 mm x 10 mm x 10 mm, were obtained by cutting, after which there were incorporated into epoxy resin, sanded and polished. For the metallographic characterization of the compounds present in the analyzed coatings structures, the surfaces were chemically attacked with Vilella reagent (a solution with 10 ml of HF, 5 ml of HNO_3, and 85 ml of H_2O) for 10 min. After preparation, the samples were analyzed with the help of the SEM microscope.

Figure 12 presents two representative SE (secondary electron) images of the 97MXC deposits, obtained by arc spray process (I - 220 A), at different values of the compressed air pressure passing through the primary circuit: $p_{primary\ air}$ = 5.5 bar; and $p_{primary\ air}$ = 6.5 bar.

The deposits from **Figure 12** present a heterogeneous microstructure formed by flattened lamellas (usually called splats), oriented parallel to the substrate, polygonal formations, unmelted spherical particles and pores - being specific microstructure to the deposits obtained by arc spray process. In the cross section of the samples are observed several variations of the structural elements brightness (various shades of gray), an aspect that suggests the inhomogeneity of the chemical composition.

XRD patterns, EDX analyses and SE images allow the identification of the various phases of the coatings. Thus, the matrix formed by light gray metal splats corresponds to FeCr and FeW phases, the dark gray flattened splats correspond to hard Fe_2B phases, at the limit of the splats some interstitial oxides appear and the areas with dark contrast correspond to the pores.

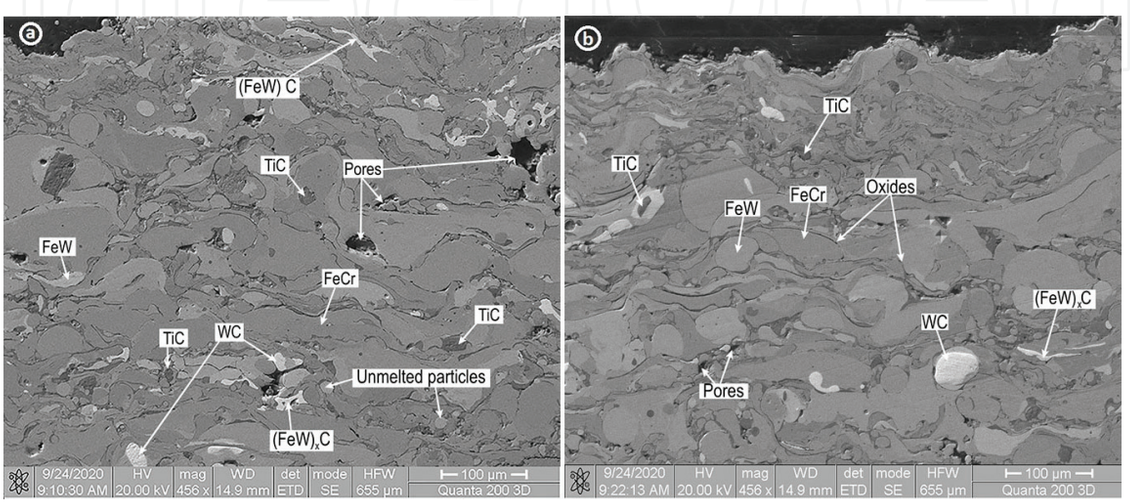

Figure 12.
SEM images of 97MXC coatings obtained under the following conditions, I = 220A, SOD = 110 mm, U = 32 V: (a) $p_{primary\ air}$ = 5.5 bar; (b) $p_{primary\ air}$ = 6.5 bar.

In the micrographs taken on the cross section, light-colored and bright polygonal formations appear, which correspond to the W-rich hard phase (WC) embedded in a matrix composed of eta type carbide $(FeW)_xC$ of light gray color. There are also present some dark gray polygonal formations which corresponds to titanium carbide (TiC). W-rich alloyed areas have a heterogeneous distribution, and inside them are formed eutectic phases of WC and W_2C type - similar to the results reported by Tillmann et al., [44].

It can be observed that at low values of the compressed air pressure passing through the primary circuit - see **Figure 12a**, in the deposit are obtained particles of larger dimensions, compared to the particle sizes presented in **Figure 12b**, which have a flattened shape. This aspect is explained by the fact that by increasing the pressure of the compressed air, the speed of the gas jet and implicitly the impact speed of the particles increase. The presence of a small quantity of unmelted particles inside the coating suggests that the temperature of the particles at the impact moment together with the spray distance were optimally chosen.

These aspects are confirmed by the investigations performed at the interface between the W-rich eutectic carbides (WC) and the metallic matrix based on Fe - see **Figure 13**. The deposits obtained at high values of electric current intensity present, around the polygonal eutectic carbides, at the interface between the W-rich phase and the Fe-based matrix, some transition areas (the luminous phase to darkness), presented in **Figure 13a,c**. The EDX analyses carried out in the dark area indicate the presence of a zone rich alloyed in Fe.

We found that the width of the transition area decreases until it disappears with the decrease of the current intensity that supplies the electric arc during the

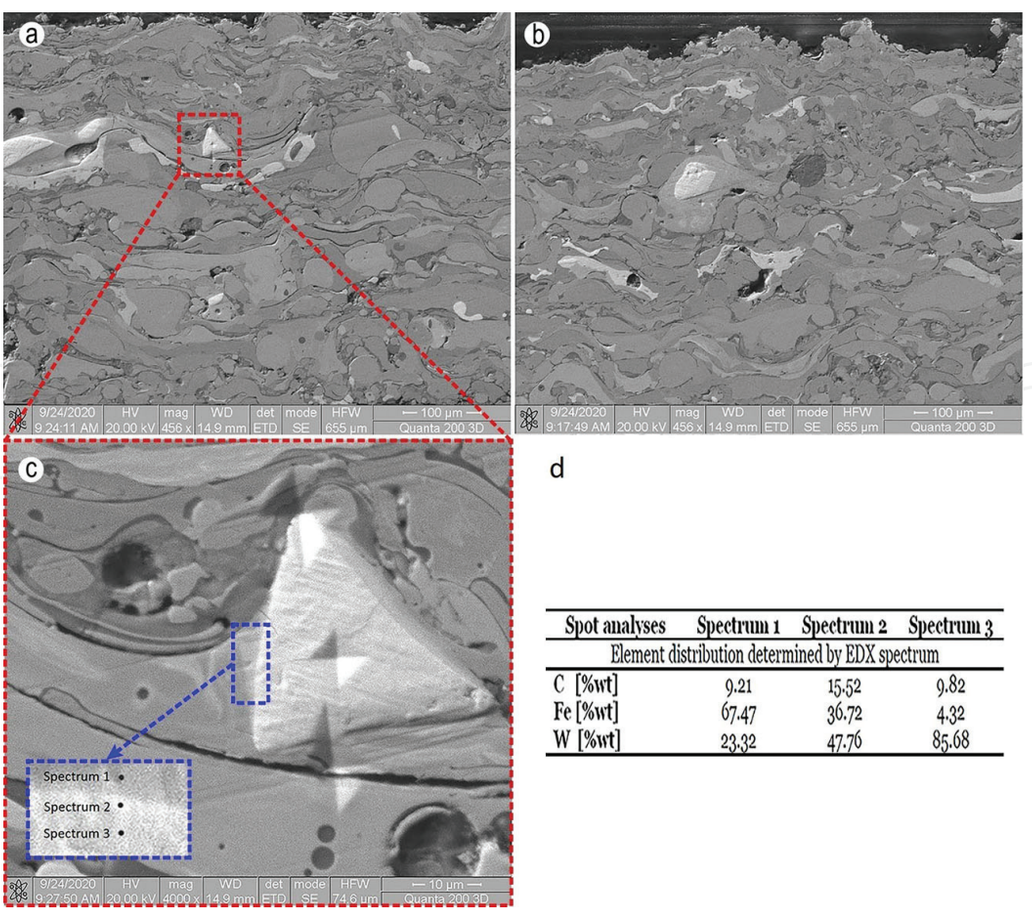

Spot analyses	Spectrum 1	Spectrum 2	Spectrum 3
Element distribution determined by EDX spectrum			
C [%wt]	9.21	15.52	9.82
Fe [%wt]	67.47	36.72	4.32
W [%wt]	23.32	47.76	85.68

Figure 13.
Cross-section images taken by SEM microscopy showing the embedment polygonal carbide WC at $p_{air\ secundary}$ = 6.5 bar: (a) I = 250A; (b) I = 200A; (c) detail figure a; (d) EDX spot analysis.

spraying process. As an example, in **Figure 13b** is presented polygonal WC carbide - where the absence of the transition zone is observed.

It can be observed that the W content decreases and the Fe amount increases in the transition area, as the distance to the eutectic polygonal carbide increases (see **Figure 13d**). These aspects suggest the fact that, by increasing the temperature of the sprayed particles and due to the increase of the electric arc intensity, the appearance of a transition zone between the polygonal eutectic carbides' WC type and the metallic matrix is favored. It can be suggested that high particle temperatures permit a better integration of the unmelted polygonal eutectic carbides into the matrix of Fe.

2.2.4 Microhardness of the 97MXC coatings

The hardness is the capacity of a piece to oppose the tendency to destroy the surface coatings by another piece, which acts on it with localized pressures on very small areas. In determining the hardness of materials, account shall be taken of the size of the traces produced by a penetrating piece, characterized by a certain shape and size and of the force acting on it. The hardness of a material is appreciated by the value of some conventional characteristics, obtained after some non-destructive tests.

Because the porous structure of the sprayed coatings does not permit the exactly determination of the hardness by conventional methods, in order to carry out investigations regarding the micro-hardness of the 97MXC deposits, we considered that the most suitable method is the Vickers method. The microhardness represents the Vickers hardness of some elements from the metallographic structure (phases, structural constituents, inclusions, etc.) and of some very thin coatings. The Vickers microhardness values presented in our study were determined using the CV - 400DAT digital microdurimeter, produced by CV Instruments, with a 100 g load, for 10s.

In order to establish the microhardness of the 97MXC coatings, we performed 5 determinations in points located at a minimum distance of 0,5 mm from each other, arranged on the transverse direction of the coating - according to the norm SR EN ISO 14923/2004.

The average values of the microhardness of the 97MXC deposits, produced in different experimental conditions are presented in **Figure 14**.

As the data presented in **Figure 14** show, the micro-hardness of 97MXC coatings is relatively high. This aspect is due both to the phases, rich alloyed in W or Ti and to the chemical compounds based on Fe_2Cr or of the eta type carbide $(FeW)_xC$ - which

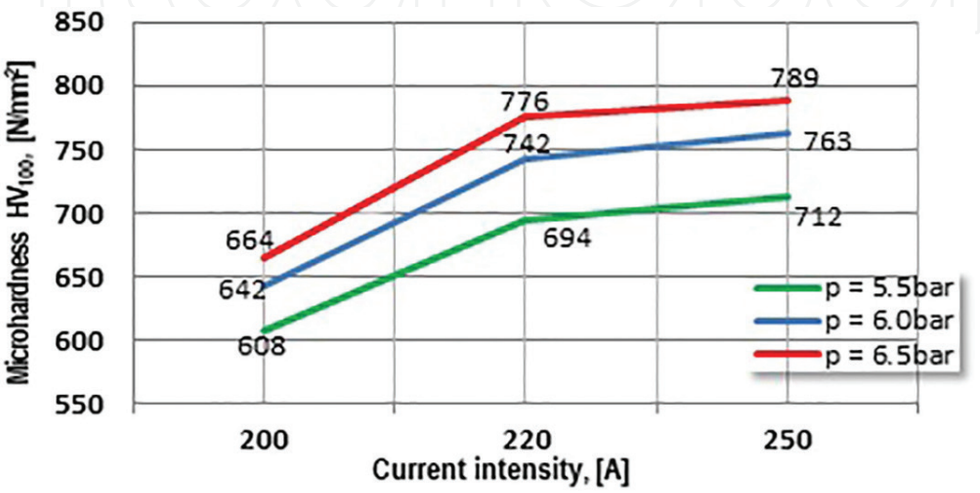

Figure 14.
HV_{100} microhardness of 97MXC coatings.

microhardness is relatively high. However, it is observed that the micro hardness of the 97MXC coatings varies in limits of up to 125 units with the pressure of the compressed air passing through the primary circuit and with the intensity of the spray current. Thus, for low values of the electric current intensity, the microhardness of the deposits is relatively low of HV_{100} = 664 ± 42 N/mm^2 compared to the microhardness of the depositions obtained at values of the electric current intensity higher than HV_{100} = 789 ± 32 N/mm^2. It can be affirmed that the high degree of homogeneity of depositions obtained at high values of the electric current intensity determines the increase of the microhardness of 97MXC deposits.

Microhardness investigations were also performed on the W, Ti and Cr hard phases. In **Figure 13b** and **c** are presented traces of the Vickers penetrator produced on the W-rich phase, in the area of the Fe phase highly alloyed with W and C (at interface) - **Figure 13b**, as well as in the low alloyed Fe phase - **Figure 13b**.

For the light-colored phases, the average microhardness value was 2842 N/mm^2, and inside the Fe-rich phase, the average microhardness value was 473 N/mm^2. At the interface level, the average microhardness value was 1387 N/mm^2. The TiC–rich phases had an average microhardness of 845 N/mm^2, the Cr-rich phases had an average microhardness of 636 N/mm^2 and those of interstitial oxides (the dark phase, positioned between the flattened particles) had an average microhardness of 258 N/mm^2. It can be suggested the fact that the transition phase, formed at the interface level between the W-rich eutectic phase and the metal matrix, rich alloyed in Fe, obtained the increasing the electric arc intensity, contains complex compounds based on Fe, W and C of $(FeW)_xC$ type, whose hardness is relatively high.

2.2.5 The wear behavior of the 97MCX ultra hard coatings

The wear behavior of the 97MCX coatings was evaluated by sliding wear tests conducted on an Amsler type system.

A general view of the AMSLER machine is given in **Figure 15**. The AMSLER machine was equipped with a data acquisition system based on tensometric strain gauges system [45], calibrated by deadweights method. The interface of the data acquisition system was realized in LabVIEW program [46]. The coated parallelepiped sample on rotating steel disc testing arrangement is presented detail.

Each coated sample was tested twice: at 20 N and 40 N normal load. The speed of the disk was kept constant, N = 100 rpm. The testing time was 3600 s. No lubricant was used. Before each test, samples were cleaned with acetone.

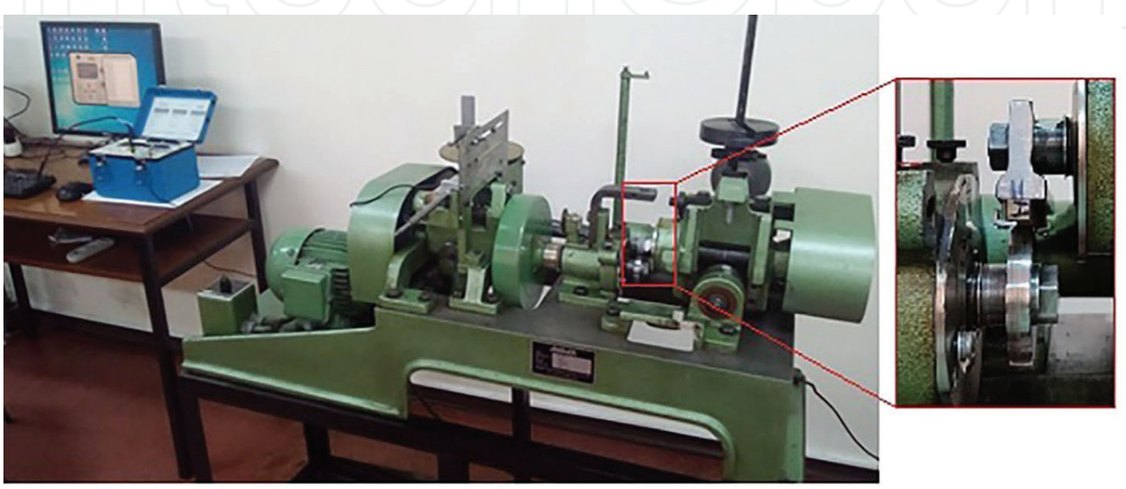

Figure 15.
General view of testing machine.

The tests were performed on three samples of 97MXC coatings obtained by arc spraying process, at pressure p = 6.5 bar and at different values of electric current intensity– see **Table 4**. The turning disk used in tribological tests was made of AISI52100 steel, hardness 64 HRC. The roughness of the tested samples was measured on Taylor-Hobson profilometer. The values of the roughness on longitudinal and transversal direction of tested samples are given in **Table 4**.

Figures 16 and **17** show the time variations of the friction coefficient and the friction torque at loads of 20 N, respectively 40 N.

The mean values of the coefficient of friction (CoF), as well as the weight loss of the samples after performing the tests at loads of 20 N and 40 N are shown in **Table 5**.

Sample	P_1 I = 200A	P_2 I = 220A	P_3 I = 250A	Disk AISI 52100
Longitudinal roughness, Ra [μm]	14.91	14.35	14.26	0.83
Transversal roughness, Ra [μm]	14.42	14.66	14.78	1.28

Table 4.
Roughness of the tested samples.

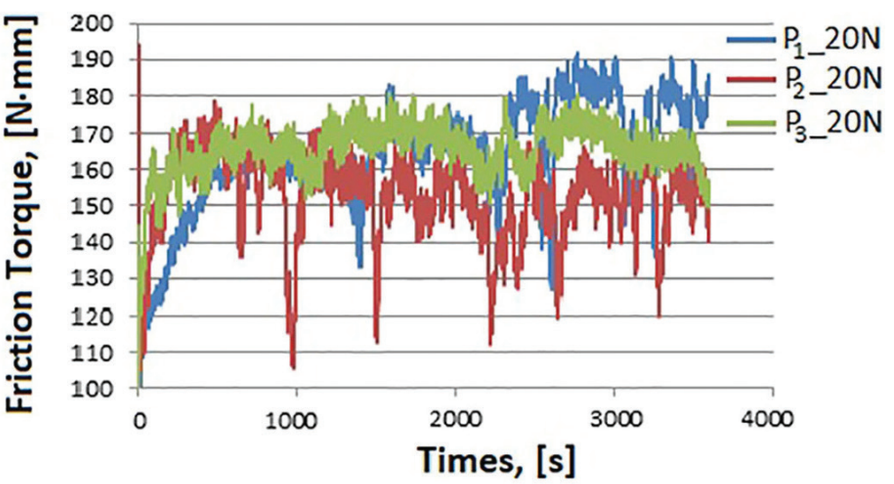

Figure 16.
Friction torque versus time at 20 N.

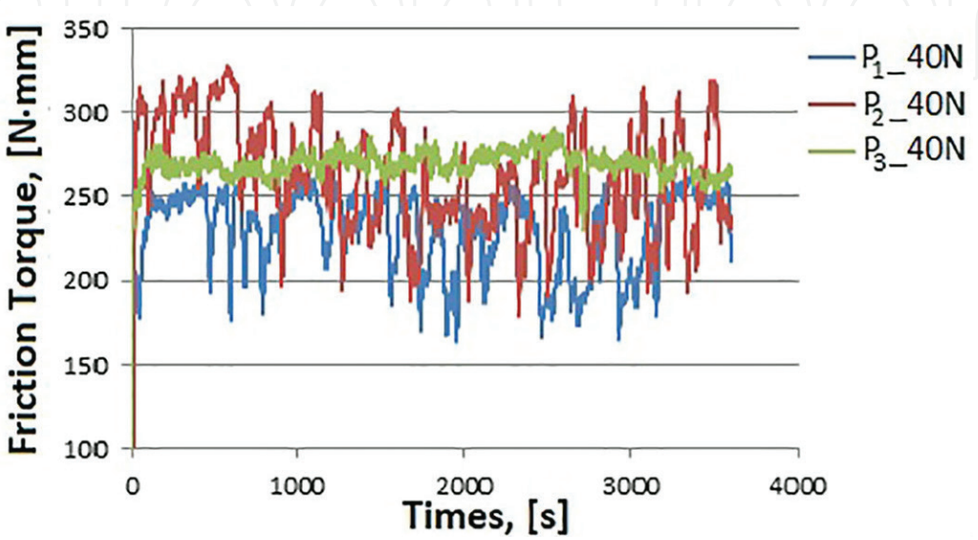

Figure 17.
Friction torque versus time at 40 N.

	Mean friction coefficients CoF					
Sample	**P_1**		**P_2**		**P_3**	
Load [N]	20	40	20	40	20	40
CoF	0.217	0.207	0.215	0.226	0.242	0.237
Wear, [%wgt]	0.000	0.028	0.000	0.004	0.000	0.011
Initial mass, g	28.976	28.976	47.874	47.855	47.226	47.226
Final mass, g	28.976	28.968	47.874	47.853	47.226	47.221

Table 5.
Mean CoF and wear in wt%.

Analyzing **Figures 16** and **17**, one can be observed that the friction torque in tribological system was more constant for P_3 sample, especially at high load - **Figure 17**). Correlated with the wear rate and general friction coefficients (CoF) results from **Table 5**, it can be concluded that the P_3 coating assure an almost constant CoF during an hour of continuous testing, while the friction torque of P_1 and P_2 manifested between large limits.

The data presented in **Table 5** show that the CoF values do not vary much by increasing the applied load, respectively from 20 N to 40 N. The average CoF values of the samples were as follows: CoF ≈ 0.21 for P1; CoF ≈ 0.22 for P2; CoF ≈ 0.24 for P_3. The CoF varied according to the quality of the tested surfaces of samples, but also with possible increase in temperature over the pad on disk contacts. A higher and constant CoF was obtained for the P_3 sample, especially at high load – see **Figure 17**.

The superior friction behavior of the P_3 against P_1 and P_2 coatings, given by the stability of the friction torque and the low wear rate, can be explained by the presence inside the deposit of the transition area between the W-rich hard phase and the $(FeW)_xC$ eta type carbide matrix, which allows fixing and maintaining the hard phase in conditions of advanced wear for a long time.

2.2.6 Analysis of 97MXC coatings adhesion

The adherence of the deposits obtained by thermal spraying is defined as being the force necessary detaching the layer from the substrate. The studies carried out by Haraga et al. [47] have demonstrated that the adhesion of the coatings is predominantly mechanical and is due to the solidification of the sprayed liquid particles or to the deformation of the semi-viscous particles on the substrate asperities. The adhesion of the deposits was determined by the traction test - in accordance with EN 582.

Figure 18 presents the adhesion variation of the deposits with the pressure of the compressed air passing through the primary circuit. It is noticed that at low values of the compressed air pressure the layer adhesion to substrate has low values. It can observe that for the same value of the compressed air pressure which passes through the primary circuit adhesion values of the deposit vary with the current intensity.

Thus, for the same pressure value, the adhesion of the 97MXC coatings obtained at I = 250A is superior to the one of the other coatings obtained at I = 200A and I = 220A, in the same technological conditions. Knowing that by the increasing of the current intensity of the electric arc temperature increases, we can suggest that, at high values of the current intensity, the drop formed in the electric arc is atomized into small particles with reduced inertia. Studies carried out by Toma et al. [33], have demonstrated that the high pressure of the compressed air favors the

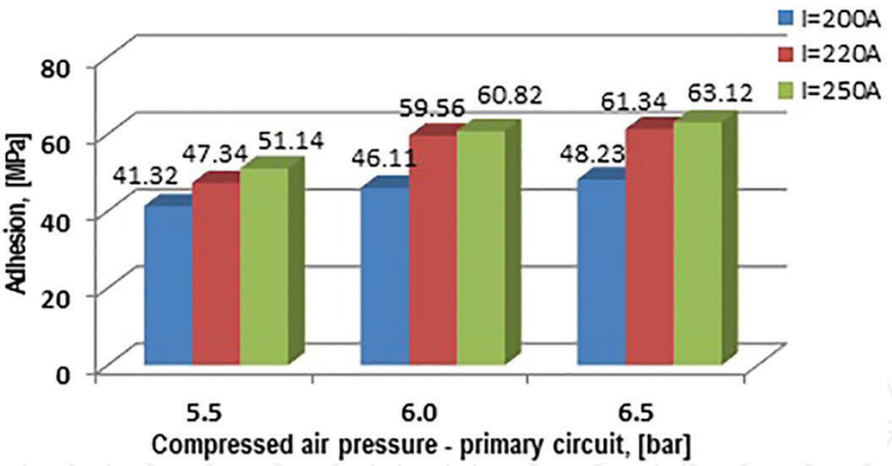

Figure 18.
Variation in the adhesion of 97MXC deposits with the compressed air pressure passing through the primary circuit.

increase of the impact velocity of the particles with the substrate surface, respectively their better fixation in the surface roughness. This aspect determines the increasing the adhesion of the 97MXC deposits with the increase of the compressed air pressure.

2.2.7 Porosity measurements of the 97MXC coatings

Porosity is a defining physical characteristic of the deposits obtained by thermal spray, due to the presence of interlamellar voids and interconnection channels between them. It is expressed by the degree of porosity of the deposit, measured in percentages, [48]. In the case of the 97MXC coatings, the porosity was investigated by image analysis of the transversal section of the specimens, using the IQ Materials software (Japan).

In **Figure 19** it is presented the variation of the average porosity of the 97MXC deposits with the compressed air pressure passing through the primary circuit - for different values of the current intensity that supplies the electric arc.

As expected, the variation of the average porosity of the 97MXC coatings presents a decreasing tendency both by the increasing of the compressed air pressure value and by the increasing of the current intensity value. Thus, it is observed that

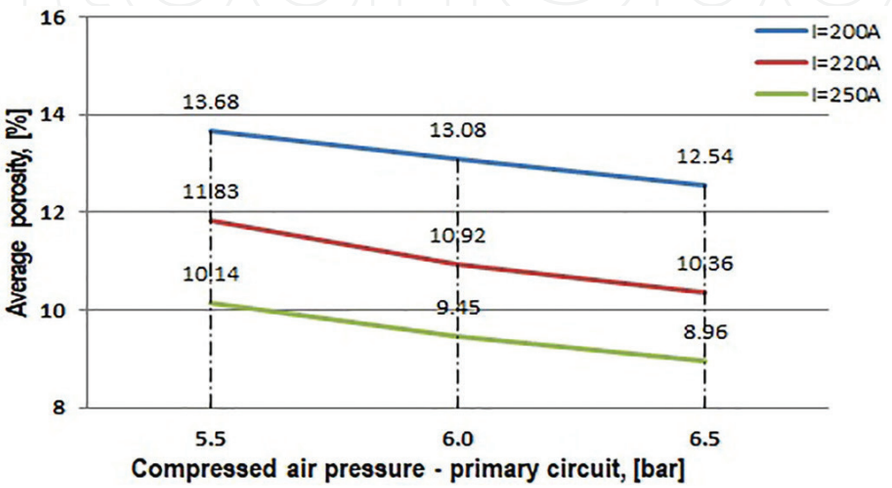

Figure 19.
Average porosity variation of 97MXC coatings with the compressed air pressure.

for the same value of the intensity of the electric current, when the compressed air pressure increases, the average porosity of the deposits decreases by up to 12%. The effect of increasing the temperature of the arc achieved by increasing the electric current determines the reduction of the average porosity by a maximum of 28%. It can be stated that between the two process parameters: compressed air pressure and electric current intensity, the latter has a "dramatic" influence on the deposition density of 97MXC.

3. Conclusions

The studies, carried out in this paper, demonstrate that qualitative deposits of hard alloys, containing WC and TiC, can be obtained by arc spray process, using a classic spray device equipped with a conical nozzle system.

The increase of the electric arc temperature, due to the increase of the current intensity favors the decomposition of some chemical compounds (TiC, FeB, WC), respectively the appearance of hard chemical compounds of type W_2C and of complex carbides of type eta: FeW_3C, Fe_3W_3C and Fe_6W_6C; the accentuated melting of the additional material and the formation of small particles with low inertia, capable to fix in the surface roughness determine the increase of the adhesion of the deposits of hard alloys and the reduction of the porosity in relatively large limits (up to 28%).

The pressure of the compressed air passing through the primary circuit determines the increase of the velocity of the sprayed particles [33], respectively their better fixation in the asperities of the substrate surface. This aspect justifies the adhesion increasing, the average porosity reducing of the coatings (by up to 12%), and the increasing of the microhardness of the coatings - at the increasing of the compressed air pressure.

The presence, inside the coatings of hard chemical compounds, type WC and W_2C - incorporated in the carbide matrix $(FeW)_xC$, as well as compounds TiC, FeCr, and FeB, permits improving the wear behavior of deposits, underlined through the stability of the friction torque, the increasing of the coefficient of friction and obtaining a low wear rate.

Conflict of interest

The authors declare no conflict of interest.

Author details

Stefan Lucian Toma[1*], Radu Armand Haraga[1], Daniela Lucia Chicet[2], Viorel Paleu[3] and Costica Bejinariu[1]

1 Department of Materials Engineering and Industrial Safety, Faculty of Materials Science and Engineering, Gheorghe Asachi Technical University of Iasi, 700050 Iasi, Romania

2 Materials Science Department, Materials Science and Engineering Faculty, Gheorghe Asachi Technical University of Iasi, 700050 Iasi, Romania

3 Mechanical Engineering, Mechatronics and Robotics Department of Mechanical Engineering Faculty, Gheorghe Asachi Technical University of Iasi, 700050 Iasi, Romania

*Address all correspondence to: stefan-lucian.toma@academic.tuiasi.ro

IntechOpen

References

[1] Sacriste D., Goubot N., Dhers J., Ducos M., and Vardelle A., An evaluation of the electric arc spray and (HPPS) processes for the manufacturing of high power plasma spraying MCrAlY coatings, J. Therm. Spray Technol., 2001, **352**, p 35-358.

[2] Pawlowski L., in: 2nd ed., The Science and Engineering of Thermal Spray Coatings, Ed. Wiley, Chichester, England, 2008.

[3] Toma B F, Baciu R E, Bejinariu C, Cimpoieșu N, Ciuntu B M, Toma S L, Burduhos-Nergis D P and Timofte D, Researches on the improvement of the bioactivity of tio2 deposits, obtained by magnetron sputtering – DC, IOP Conf. Series: Mat. Science and Engineering, 2018, 374: 012017.

[4] Newbery, A.P., Grant, P.S., Neiser, R.A., The velocity and temperature of steel droplets during electric arc spraying, Surf. Coat. Technol. 195 (2005) 91-101.

[5] Bémer, D., Subra, I., Morele, Y., Charvet, A., Thomas, D., Experimental study of granular bed filtration of ultra fine particles emitted by a thermal spraying process, Journal of AerosolScience 2013, 63:25-37.

[6] Toma SL, Bejinariu, C, Gheorghiu, DA, Baciu, C, The improvement of the physical and mechanical properties of steel deposits obtained by thermal spraying in electric arc, Advanced Materials Research, 2013, 814, 173-179, DOI: 10.4028/www.scientific.net/AMR.814.173.

[7] Katranidis V., Kamnis S., Allcock B., Gu S., Effects and interplays of spray angle and stand-off distance on the sliding wear behavior of HVOF WC-17Co coatings, J Therm Spray Tech, 2019, 28, pp. 514-534.

[8] Audisio, S., Caillet, M., Galerie, A. and Mazille, M., Préparation d'une Surface (Surface Preparation), Traitements de Surface et Protection contre la Corrosion (Surface Treatments and Protection against Corrosion), Les Éditions de Physiques, Paris, France, 1987, p 169-174

[9] Toma S.L., Bejinariu C., Eva L., Sandu I.G., Toma B.F., Influence of process parameters on the properties of TiO_2 films deposited by a D.C. magnetron sputtering system on glass support, Key Engineering Materials, 2015, 660: 86-92.

[10] Tillmann W., Walther F., Luo W.F., Haack M., Nellesen J., Knyazeva M., In Situ Acoustic Monitoring of Thermal Spray Process Using High-Frequency Impulse Measurements, J. of Therm. Spray Technol., 2018, 27: 50-58.

[11] St. Toma, Contribution Regarding the Steels Metallization Through Activated Thermal Spraying, PhD Thesis, Gheorghe Asachi Technical University Iasi, Romania, 2009.

[12] Zimmermann, S., Gries, B., Fischer, J., Lugscheider, E. (Eds.), Thermal Spray 2008: Crossing Borders: Proceedings of the International Thermal Spray Conference 2008, DVS Deutscher Verband für Schweißen, Düsseldorf, 2008.

[13] Arif, Z.U., Shah, M., and Rehman, E., Tariq, A., Effect of spraying parameters on surface roughness, deposition efficiency, and microstructure of electric arc sprayed brass coating, International Journal of Advanced and Applied Sciences, 2020, 7(7): 25-39.

[14] Berger L.M., Saaro S., Naumann T., Wiener M., Weihnacht V., Thiele S., Suchánek J., Microstructure and properties of HVOF-sprayed chromium

alloyed WC-Co and WC-Ni coatings, Surf. Coat. Technol. 2008, Vol. 202, pp 4417.

[15] Nurisna Z.; Triyono; Muhayat N, Wijayanta, AT., Effect of layer thickness on the properties of nickel thermal sprayed steel, Book Series AIP Conference Proceedings, 2016, Vol. 1717, Art. Nr. 040012.

[16] Tillmann, W. and Abdulgader, Wire Composition: Its Effect on Metal Disintegration and Particle Formation in Twin-Wire Arc-Spraying Process, Journal of Thermal Spray Technology, 2013, 22: 352-362.

[17] http://ctwhardfacing.co.uk/celcoat-services/wire-arc-spray-coatings/(Accesed: 05.10.2020)

[18] Toma S.L, The influence of jet gas temperature on the characteristics of steel coating obtained by wire arc spraying, Surf & Coat. Technol., 2013, 220:261-265.

[19] Z. Lu, J. Cao, H.F. Lu, L.Y. Zhang, K.Y. Luo, Wear properties and microstructural analyses of Fe-based coatings with various WC contents on H13 die steel by laser cladding, Surface & Coatings Technology, 2019, 369: 228-237.

[20] Tillmann, W., Luo, W., Selvadurai, U., Wear analysis of thermal spray coatings on 3D surfaces, J. Therm. Spray Technol. 2014, 23: 245-251.

[21] Toma S.L., Badescu M., Ionita I., Ciocoiu M. and L. Eva, Influence of the Spraying Distance and Jet Temperature on the Porosity and Adhesion of the Ti Depositions, Obtained by Thermal Spraying in Electric Arc - Thermal Activated, Applied Mechanics and Materials, 2014, 657: 296-300.

[22] Planche MP, Liao H, Coddet C, Relationships between in-flight particle characteristics and coating microstructure with a twin wire arc spray process and different working conditions, Surf & Coat. Technol., 2004, 220: 215-226.

[23] Gedzevicius I, Valiulis AV Analysis of wire arc spraying process variables on coatings properties, Analysis of wire arc spraying process variables on coatings properties, 2006, 175:206-211.

[24] Cazac, A.M., Bejinariu, C., Ionita, I., Toma, S.L., Rodu, C., Design and Implementation of a Device for Nanostructuring of Metallic Materials by Multiaxial Forging Method, Applied Mechanics and Materials, 2014, 657: 193-197, DOI: 10.4028/www.scientific.net/AMM.657.193.

[25] Sharifahmadian O, Salimijazi HR, Fathi MH, Mostaghimi J, Pershin L, Relationship between surface properties and antibacterial behavior of wire arc spray copper coatings Surf & Coat. Technol., 2013, 233: 79-79.

[26] Toma SL, Gheorghiu DA, Radu S, Bejinariu C, The influence of the diffusion on adherence of the 60T deposits obtained through thermal spraying in electric arc, Applied Mechanics and Materials, 2013, 371: 193-197, DOI: 10.4028/www.scientific.net/AMM.657.193.

[27] Zhao XY, Xiang, M, Zhou HC, Zhang WH, Numerical Investigation and Analysis of the Unsteady Supercavity Flows with a Strong Gas Jet, Journal Of Applied Fluid Mechanics, 2020, 13, 1323-1337.

[28] Masoumeh, G., Shahrooz, S., Mahmood, G., Ahmad, S. E., Investigation of stand-off distance effect on structure, adhesion and hardness of copper coatings obtained by the APS technique, J. Theor Appl Phys, 2018, 12, 85-91.

[29] Grigorenko GM, Adeeva LI, Tunik AY, Korzhik VN, Doroshenko LK,

Titkov YP, Chaika AA, Structurization of coatings in the plasma arc spraying process using B4C + (Cr, Fe)(7)C-3-cored wires, Powder Metallurgy and Metal Ceramics, 2019, 58:312-322.

[30] Giovanni Bolelli, Alberto Colella, Luca Lusvarghi, Stefania Morelli, Pietro Puddu, Enrico Righetti, Paolo Sassatelli, Veronica Testa, 2020, TiC–NiCr thermal spray coatings as an alternative to WC-CoCr and Cr3C2–NiCr, Wear, 450-451, 203273.

[31] Haraga, R.A., Bejinariu, C., Cazac, A., Toma B.F, Baciu, C., Toma, St.L. 2019, Influence of surface roughness and current intensity on the adhesion of high alloyed steel deposits - obtained by thermal spraying in electric arc, IOP Conference Series: Materials Science and Engineering, 572, DOI:10.1088/1757-899X/572/1/012056.

[32] Toma SL, Savin G, Toma BF, Bejinariu C, Ionita I, Vizureanu P, Badaru G, Sandu AV, Cazac a, Burduhos ND, System of concentric nozzles for metal spraying guns for drawable metallic materials, has conical stiffening shoulder that is provided on conical nozzle, inclined under angle relative to longitudinal axis of conical nozzle, Gheorghe Asachi Technical University Iasi, Patent Number RO134208-A2, 2020.

[33] Toma SL, Bejinariu C, Baciu R, Radu S. The effect of frontal nozzle geometry and gas pressure on the steel coating properties obtained by wire arc spraying, Surf & Coat. Technol., 2013, 220. DOI.org/10.1016/j.surfcoat.2012.11.011.

[34] Bejinariu C, Munteanu C, Florea CD, Istrate B, Cimpoesu N, Alexandru A, Sandu AV, Electro-chemical Corrosion of a Cast Iron Protected with a Al2O3 Ceramic Layer, Revista de chimie, 2018, 69(12): 3586-3589.

[35] Coddet, C., Montavon, G., Ayrault-Costil, S., Freneaux, O., Rigolet, F., Barbezat, G., Folio, F., Diard, A. and Wazen, P., Surface Preparation and Thermal Spray in a Single Step: The PROTAL Process—Example of Application for an Aluminum-Base Substrate Journal of Thermal Spray Technology,1999, 8(2): 235.

[36] Wigren, J., Grit Blasting as Surface Preparation before Plasma Spraying, Surf. Coat. Technol., Vol 34, 1988, p 101-108.

[37] Chicet D., Tufescu A., Paulin C., Panturu M., Munteanu C., The Simulation of Point Contact Stress State for APS Coatings, IOP Conference Series: Materials Science and Engineering, 2017, 209, 17578981.

[38] Calin, MA; Curteza, A; Toma, S, Agop, M, Morphological properties of polyamide 6-cnt nanofibers obtained by electrospinning method, Metalurgia International, 2013, 18: 19-22.

[39] Gray, H., Wagner, L. and Lütjering, G., Influence of Surface Treatment on the Fatigue Behavior of Ti-Alloys at Room and Elevated Temperatures, Sixth World Conference on Titanium, P. Lacombe, R. Tricot, and G. Béranger, Ed., Les Éditions de Physique, Paris, France, 1998, p 1895-1900.

[40] Paulin C., Chicet D.L., Istrate B., Panturu M., Munteanu C., Corrosion behavior aspects of Ni-base self-fluxing coatings, IOP Conference Series: Materials Science and Engineering, 2016, 147, 17578981.

[41] Nanu, C, Poeata, I, Popescu, C; Eva, L; Toma, BF; Toma, SL, The Influence of the Characteristics of Plastic Materials Used in the Performance of the Thoraco-Lumbar Orthoses, Materiale Plastice, 2018, 55: 85-90.

[42] Panturu M., Chicet D., Paulin C., Lupescu S., Munteanu C., 2017,

Microstructural aspects of TBC's deposited on internal combustion engine valve materials, Materials Science Forum, 907, 02555476.

[43] He, D.J., Fu, B.J., Jiang, J.M., Li, X.J., Microstructure and wear performance of arc sprayed Fe-FeB-WC coatings, J. Therm. Spray Technol. 17 (2008) 757-761.

[44] Tillmann, W., Hagen, L., Kokalj, D., Embedment of eutectic tungsten carbides in arc sprayed steel coatings, Surface & Coatings Technology, 2017, 331:153-162.

[45] Paleu, V., Georgescu, S., Baciu, C., Istrate, B., & Baciu, ER. Preliminary experimental research on friction characteristics of a thick gravitational casted babbit layer on steel substrate. IOP Conference Series: Materials Science and Engineering, 2016, 147, 012028. doi:10.1088/1757-899x/147/1/012028.

[46] Paulin, C., Chicet, D., Paleu, V., Benchea, M., Lupescu, Ş., & Munteanu, C. Dry friction aspects of Ni-based self-fluxing flame sprayed coatings. IOP Conference Series: Materials Science and Engineering, 2017, 227, 012091. doi:10.1088/1757-899x/227/1/012091.

[47] Haraga, R.A., Chicet Dl, Cimpoiesu N, Toma SL, Bejinariu C. Influence of the Stand-off Distance and of the Layers Thickness on the Adhesion and Porosity of the 97MXC Deposits Obtained by Arc Spraying Process, IOP Conference Series: Materials Science and Engineering, 2020, 877(1)/ DOI:10.1088 / 1757-899X / 877/1/012020.

[48] Bejinariu, C, Burduhos-Nergis, DP, Cimpoesu, N, Bernevig-Sava, A, Toma, SL, Study on the anticorrosive phosphated steel carabiners used at personal protective equipment Quality-access to success, 2019, 20: 71-76 Supplement 1.